Topological Changes in Periodicity Hubs of Dissipative Systems

Roberto Barrio,[1,*] Fernando Blesa,[2] and Sergio Serrano[1]
[1]Departamento de Matemática Aplicada and IUMA, University of Zaragoza, E-50009, Spain
[2]Departamento de Física Aplicada, University of Zaragoza, E-50009, Spain
(Received 16 December 2011; revised manuscript received 23 March 2012; published 25 May 2012)

We reveal the existence of a new codimension-1 curve that involves a topological change in the structure of the chaotic invariant sets (attractors and saddles) in generic three-dimensional dissipative systems with Shilnikov saddle foci. This curve is related to the spiral-like structures of periodicity hubs that appear in the biparameter phase plane. We show how this curve configures the spiral structure (via the doubly superstable points) originated by the existence of Shilnikov homoclinics and how it separates two regions with different kinds of chaotic attractors or chaotic saddles. Inside each region, the topological structure is the same for both chaotic attractors and saddles.

DOI: 10.1103/PhysRevLett.108.214102 PACS numbers: 05.45.Ac, 05.45.Pq

Periodicity hubs are spiral-like structures in the biparameter space formed by shrimp-shaped regular regions connected to the focal point of a spiral structure [1]. Their organizing centers have been recently connected to the existence of Shilnikov homoclinics near a codimension-2 bifurcation of saddle foci [2].

Shrimp-shaped regular regions were initially studied in [3,4] for a Rössler model by using maps that reproduce many of the observed phenomena. Subsequently, these regions have been studied in numerous problems both in maps [5] and in time-continuous systems [1,6], and they have also been observed experimentally [7,8]. Therefore, it is an important phenomenon for both theoretical and applied studies.

Most of these systems are strongly dissipative, and the contraction of the flow along the stable manifolds is much greater than the expansion along the unstable manifolds of the equilibria [9,10]. Thus, these systems accept a qualitative description through one-dimensional maps [4]. The standard way to obtain such maps is to compute the Poincaré First Return Map (FRM) of the attracting invariant sets. However, when these sets are just periodic orbits with period p, only p points appear in the FRM. Some authors [8] studied that case experimentally and numerically using the FRM in chaotic regions near the borders of shrimp-shaped regular regions. Instead, we propose to go further and to use all the chaotic invariant structures of the system, either chaotic attractors or chaotic saddles, and not just the attracting objects. In [2], a curve of change of topology of the chaotic attractors was detected, but this curve was not connected to the shrimp structures. In this Letter, the FRM of all the chaotic invariants is obtained in the whole biparametric plane—that is, on the chaotic regions and on the shrimp-shaped regular regions. This method allows us to obtain a natural one-dimensional biparameter family of maps in the entire periodicity hub and to show that such a region is completely separated into two well-defined parts depending on the topological structure of its chaotic invariant sets, whether the sets are chaotic attractors or saddles. Moreover, the results show that all of the chaotic invariant sets have the same topological structure on the same regions.

As an example, we use the canonical Rössler system [11]:

$$\dot{x} = -(y+z), \quad \dot{y} = x + ay, \quad \dot{z} = b + z(x-c), \tag{1}$$

with two bifurcation parameters a and c (we fix $b = 0.2$). Figure 1 shows a biparametric Lyapunov spectrum diagram. Colors discriminate between the regions of regular and chaotic dynamics corresponding, respectively, to a zero and positive maximal Lyapunov exponent λ_1. A good choice for the section of the FRM [9] is $\Sigma = \{(x,y,z) \in \mathbb{R}^3 | x = x_-, \dot{x} > 0\}$, with $x_- = (c - \sqrt{c^2 - 4ab})/2$ (the x coordinate of one of the equilibrium points). Figures 2(a) and 2(c) show chaotic attractors for

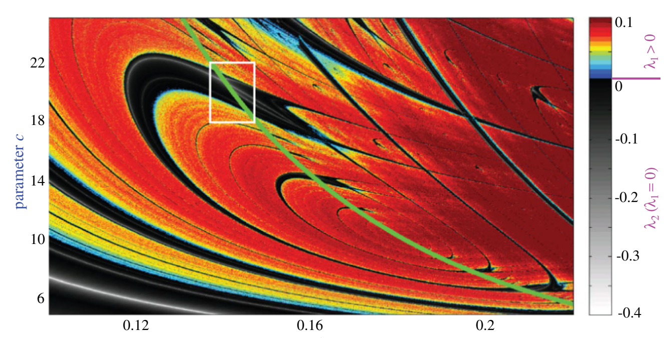

FIG. 1 (color online). Spirals and "shrimps" in a 1000×1000-grid biparametric Lyapunov diagram of the Rössler model. The color bar for the Lyapunov exponent range identifies the regions of chaotic and regular (black) dynamics. The thick curve (green) determines a change in the topological structure of the chaotic invariant set from a unimodal map (left) to a bimodal map (right). The white rectangle corresponds to the parameter region, shown in detail in Fig. 6.

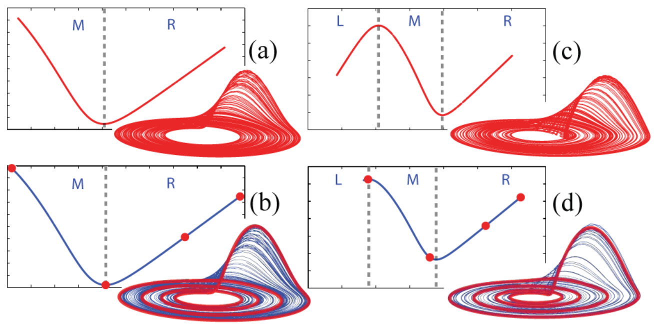

FIG. 2 (color online). Chaotic invariant sets and their FRM for different values of the parameter a ($b = 0.2$ and $c = 20$). Panels (a) and (c) correspond to chaotic attractors ($a = 0.11$ and $a = 0.2$, respectively), while (b) and (d) are chaotic saddles ($a = 0.118$ and $a = 0.149$, respectively) with the coexisting stable periodic orbits (big dots in red).

different values of parameters with different topological structures [9,11]: (a) corresponds to a "spiral-shaped attractor" with a unimodal FRM (right panel), and (c) is a "screw-shaped attractor" with a bimodal FRM. This change in the topology of the attractors has also been observed in an experimental circuit realization of the Rössler model (Fig. 3), as well as in other models [7,8].

In the regular regions there are no chaotic attractors, but transient chaos is observed. Figure 4 shows two different time series with the same values of parameters, but with two slightly different sets of initial conditions. We can see how in the first case the trajectory quickly converges to the stable periodic orbit, while in the second case the trajectory experiences a transient irregular motion for more time, until finally it converges to the same periodic orbit. In any case, transient chaos exists, and it is due to the existence of a nonattracting chaotic saddle in the phase space [12]. Using the sprinkler method [13], we may compute the chaotic saddles, and we may work with them in the same way as with the chaotic attractors in the chaotic regions. Figures 2(b) and 2(d) show two chaotic saddles with the same topological structure as the chaotic attractors in (a) and (c), respectively.

The thick green curve crossing Fig. 1 has been obtained by studying the change of topology in the chaotic invariant sets throughout the chaotic regions and periodicity hubs. We denote such a curve as the topological branch adding bifurcation curve (TBA), and it is a global codimension-1 bifurcation curve. Both chaotic attractors and saddles are composed of unstable periodic orbits and they are robust; i.e., most of the unstable periodic orbits that appear within a shrimp-shaped regular region continue to exist in the surrounding chaotic region and vice versa. So, the change of asymptotic behavior of the flow, from chaotic to regular or vice versa, does not imply a change in the topology of the chaotic invariant set, and we can check how the TBA curve smoothly crosses both chaotic and regular regions, remaining well defined throughout the entire periodicity hub.

The topological structure of the Rössler chaotic invariant sets can be described in terms of their topological template [10]—that is, a branched, two-dimensional manifold such that all periodic orbits in the invariant set can be projected onto the template without changing their knot and link invariants. Practically, the template may be derived using a FRM of the chaotic set for further examining the knots of the unstable periodic orbits foliating it. The map allows for determination of the number of branches of the template in which the twists and crossings of the unstable periodic orbits determine the topological template. On the left of the TBA-bifurcation line, the chaotic invariants (attractors or saddles) present a 1D unimodal map and, thus, a topological template with two branches. On the right, the topological template has a new branch obtained at the TBA curve, as the map is now a bimodal map. In fact, we may consider that the system has a complex topological template with all the possible options, while leaving some branches "closed," which gives a simpler template. (Figure 5 shows the generic template as obtained in [2].) But at the TBA curve, a new branch is "open" for the system and new periodic orbits can be obtained.

In the regular regions, the variation of the second Lyapunov exponent λ_2 points out superstability curves, i.e., the points in the biparameter plane where stable periodic orbits with a minimum value of λ_2 exist. If we make a magnification of a shrimp-shaped regular region (see Fig. 6), the figure shows that the TBA curve passes through

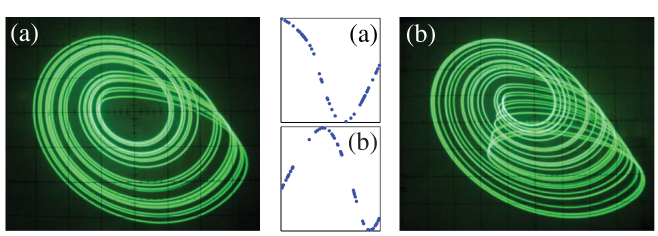

FIG. 3 (color online). Experimental chaotic invariant sets and their FRM corresponding to spiral (a) and screw (b) chaotic attractors.

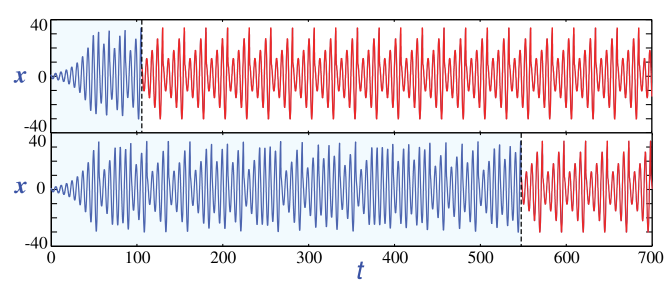

FIG. 4 (color online). Time series of two slightly different sets of initial conditions. The first part (blue) corresponds to transient chaos. In the second part (red), the trajectory has converged to the stable periodic orbit.

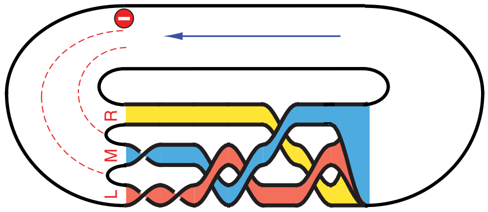

FIG. 5 (color online). Generic topological template for the complete parametric plane of Fig. 1. The forbidden branch is "open" at the TBA-bifurcation line.

the intersection point of the two main superstability curves of the shrimp. This situation was analyzed in [4], defining a model made by a biparameter family of one-dimensional maps. For a map, superstability curves correspond to the locus of the points in the parameter plane where a periodic orbit contains a critical point. If we have a bimodal map and fix a period, we can get two families of superstable orbits, one for each extremum. We denote s_+ and s_- as the superstability curves corresponding to the maximum and minimum, respectively. These two curves can cross when there is a doubly superstable orbit (the orbit contains both maximum and minimum) or when there is coexistence of two different superstable orbits.

In [1], a curve joining the doubly superstable points was shown, but it was not related to the change of the topology of chaotic sets. What we show here is that, in fact, this curve is an important object, since it divides the whole parametric plane in regions of different topology both in chaotic and regular regions. This conclusion has several remarkable consequences: the main one is that on one side of the curve we have more periodic orbits because the chaotic invariant sets need more symbols to describe the unstable periodic orbits foliated to it. In addition, the global study of the FRM permits us to relate directly the numerical results obtained in the differential system with those obtained in [4] with their simplified map model.

In Fig. 6, the surrounding panels show the FRM corresponding to existing chaotic invariant sets for different values of the parameters. In the regular region we have also obtained the map of the stable periodic orbit. We associate to each orbit a four-letter word (in this "shrimp," the main stable periodic orbits have multiplicity four) using five symbols: L, A, M, B, and R. We assign a symbol to each point of the orbit in the FRM according to its position, such that A and B represent the maximum and minimum, respectively, and L, M, and R the successive monotony intervals from left to right (Fig. 2), defined by the two extrema [14]. For example, in panel 9 of Fig. 6, *LRRB* means that the first point is on the left interval, the next two points are on the right, and the last point is at the minimum.

The stable periodic orbits with a minimum value of λ_2 (panels 3, 5, 7, 9, and 11) correspond directly to the

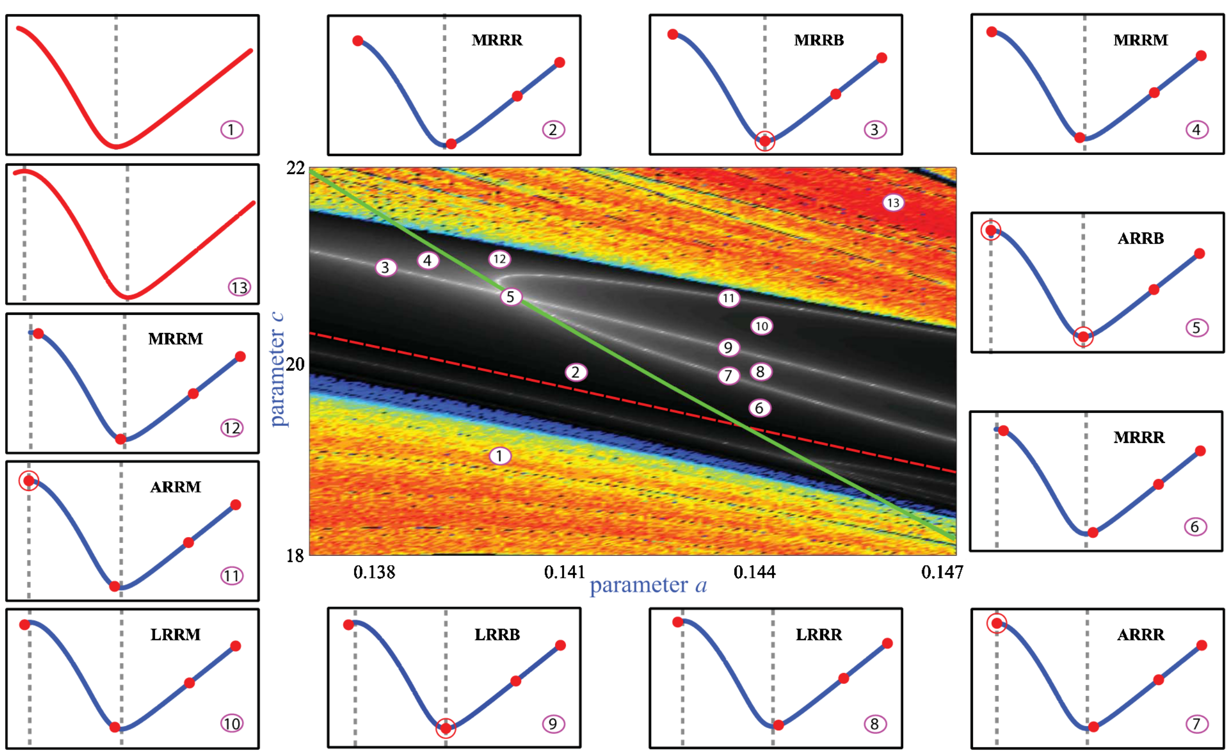

FIG. 6 (color online). Magnification of Fig. 1 in the central panel. Surrounding panels show the FRM corresponding to chaotic invariant sets of different regions delimited by the superstability curves. Red dots point out the FRM of coexisting stable periodic orbits, with the encircled ones denoting the extrema points.

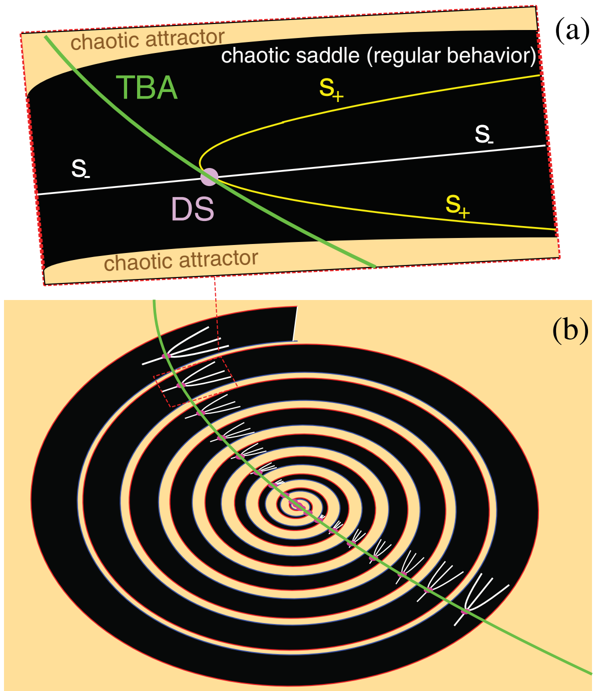

FIG. 7 (color online). Top: Sketch of superstability curves in a shrimp-shaped regular region. Bottom: Sketch of the spiral structure with the TBA curve passing across the doubly superstable (DS) points in the periodicity hub.

definition of superstable orbits for maps. The periodic orbit in panel 5, where both superstability curves cross, is a doubly superstable orbit. In addition, the map of the orbits of the curve s_- (3 and 9) pass through the local minimum of the FRM, while orbits of the (parabola-shaped) curve s_+ (7 and 11) pass through the local maximum of the FRM.

All orbits of s_- [see Fig. 7(a) for a scheme] to the left of point 5 have been assigned the word *MRRB*. As we get closer to 5, point *M* is shifted to the left; the orbit at 5 reaches *A* and orbits to the right of 5 have been assigned the word *LRRB*. Similarly, curve s_+ has two branches originating at 5; the orbits of the upper branch (*ARRM*) have the last point in *M*, and the orbits of the lower branch (*ARRR*) have the last point in *R*. The window of main periodicity (in the case of the central panel in Fig. 6, the regular region above the first period-doubling curve, shown by the dotted red line) can be divided into six subregions bounded by s_+, s_-, and the TBA curve. Also, the chaotic attractors in panels 13 and 1 have the same topology as the chaotic saddles at the shrimp-shaped regular regions on the right and left, respectively, of the green TBA curve.

From the analysis of Fig. 6, it follows that the area on the right of s_+ must be on the right of the TBA curve, because the FRM of the chaotic saddle is unimodal on the left of the curve. In fact, we can see that s_+ is tangent to the curve of change of topology at point 5 (the doubly superstable point). This tangent point acts as an organizer of the subregions described above.

We have shown that the FRMs of both chaotic saddles and chaotic attractors define a family of unidimensional maps throughout the region of influence of periodicity hubs. These maps appear naturally by the intrinsic characteristics of the flow and allow linking the results on maps with the situations observed in dissipative differential systems. In particular, we have found numerically that the curve of change of topology that divides the spiral structure around the periodicity hub passes through the main doubly superstable point of each shrimp-shaped regular region. In addition, relying on the known results about maps, we have justified that this point is a tangent point between the TBA curve and s_+. This behavior gives us the scheme of the spiral structures and organization inside the shrimps shown in Fig. 7: the TBA curve is tangent to the superstable curves s_+ at the doubly superstable (DS) points defining all the "shrimp" structures, and it is perfectly defined in the entire parametric plane by studying the topological changes of all the chaotic invariant objects.

R. B. and S. S. have been supported for this research by the Spanish Research Grant MTM2009-10767, and F. B. has been supported for this research by the Spanish Research Grant AYA2008-05572.

*Corresponding author.
rbarrio@unizar.es

[1] C. Bonatto and J. A. C. Gallas, Phys. Rev. Lett. **101**, 054101 (2008).
[2] R. Barrio, F. Blesa, S. Serrano, and A. Shilnikov, Phys. Rev. E **84**, 035201 (2011).
[3] S. Fraser and R. Kapral, Phys. Rev. A **25**, 3223 (1982); E. A. Celarier and R. Kapral, J. Chem. Phys. **86**, 3357 (1987); **86**, 3366 (1987).
[4] P. Gaspard, R. Kapral, and G. Nicolis, J. Stat. Phys. **35**, 697 (1984).
[5] M. Schell, S. Fraser, and R. Kapral, Phys. Rev. A **28**, 373 (1983); J. A. C. Gallas, Phys. Rev. Lett. **70**, 2714 (1993); Appl. Phys. B **60**, S203 (1995); M. S. Baptista and I. L. Caldas, Chaos Solitons Fractals **7**, 325 (1996); B. R. Hunt and E. Ott, J. Phys. A **30**, 7067 (1997); B. R. Hunt, J. A. C. Gallas, C. Grebogi, J. A. Yorke, and H. Koçak, Physica (Amsterdam) **129D**, 35 (1999); E. N. Lorenz, Physica (Amsterdam) **237D**, 1689 (2008).
[6] A. Hastings and T. Powell, Ecology **72**, 896 (1991); Y. A. Kuznetsov, O. De Feo, and S. Rinaldi, SIAM J. Appl. Math. **62**, 462 (2001); V. Castro, M. Monti, W. B. Pardo, J. A. Walkenstein, and E. Rosa, Jr., Int. J. Bifurcation Chaos Appl. Sci. Eng. **17**, 965 (2007); R. Barrio, F. Blesa, and S. Serrano, Physica (Amsterdam) **238D**, 1087 (2009); J. G. Freire and J. A. C. Gallas, Phys. Rev. E **82**, 037202 (2010); J. Slipantschuk, E. Ullner, M. da Silva Baptista, M. Zeineddine, and M. Thiel, Chaos **20**, 045117 (2010); J. A. C. Gallas, Int. J. Bifurcation Chaos Appl. Sci. Eng. **20**, 197 (2010); M. A. Nascimento, J. A. C. Gallas,

and H. Varela, Phys. Chem. Chem. Phys. **13**, 441 (2011); R. Vitolo, P. Glendinning, and J. A. C. Gallas, Phys. Rev. E **84**, 016216 (2011).

[7] C. Bonatto, J. C. Garreau, and J. A. C. Gallas, Phys. Rev. Lett. **95**, 143905 (2005); R. Stoop, P. Benner, and Y. Uwate, Phys. Rev. Lett. **105**, 074102 (2010).

[8] D. M. Maranhão, M. S. Baptista, J. C. Sartorelli, and I. L. Caldas, Phys. Rev. E **77**, 037202 (2008).

[9] C. Letellier, P. Dutertre, and B. Maheu, Chaos **5**, 271 (1995).

[10] R. Gilmore, Rev. Mod. Phys. **70**, 1455 (1998); G. Boulant, M. Lefranc, S. Bielawski, and D. Derozier, Int. J. Bifurcation Chaos Appl. Sci. Eng. **8**, 965 (1998); R. Gilmore and M. Lefranc, *The Topology of Chaos* (Wiley, New York, 2002); J. Used and J. C. Martín, Phys. Rev. E **82**, 016218 (2010).

[11] O. E. Rössler, Phys. Lett. **57A**, 397 (1976).

[12] C. Grebogi, E. Ott, and J. A. Yorke, Phys. Rev. Lett. **48**, 1507 (1982).

[13] H. Kantz and P. Grassberger, Physica (Amsterdam) **17D**, 75 (1985).

[14] J. P. Lampreia and J. Sousa Ramos, Portugal. Math. **54**, 1 (1997).